*Journal of Experimental Botany*, Vol. 67, No. 11 pp. 3445–3456, 2016
doi:10.1093/jxb/erw163 Advance Access publication 29 April 2016
This paper is available online free of all access charges (see http://jxb.oxfordjournals.org/open_access.html for further details)

RESEARCH PAPER

# Large variation in the Rubisco kinetics of diatoms reveals diversity among their carbon-concentrating mechanisms

**Jodi N. Young[1,*,†], Ana M.C. Heureux[2], Robert E. Sharwood[3], Rosalind E.M. Rickaby[2], François M.M. Morel[1] and Spencer M. Whitney[3]**

[1] Department of Geosciences, Princeton University, Princeton, NJ 08544, USA
[2] Department of Earth Sciences, University of Oxford, South Parks Road, Oxford OX1 3AN, UK
[3] Plant Science Division, Research School of Biology, The Australian National University, Canberra, ACT 2601, Australia

* Correspondence: youngjn@uw.edu
† Present address: Department of Oceanography, University of Washington, 1503 NE Boat St, Seattle, WA 98105, USA

Received 27 February 2016; Accepted 5 April 2016

Editor: Christine Raines, University of Essex

## Abstract

**While marine phytoplankton rival plants in their contribution to global primary productivity, our understanding of their photosynthesis remains rudimentary. In particular, the kinetic diversity of the $CO_2$-fixing enzyme, Rubisco, in phytoplankton remains unknown. Here we quantify the maximum rates of carboxylation ($k_{cat}^c$), oxygenation ($k_{cat}^o$), Michaelis constants ($K_m$) for $CO_2$ ($K_C$) and $O_2$ ($K_O$), and specificity for $CO_2$ over $O_2$ ($S_{C/O}$) for Form I Rubisco from 11 diatom species. Diatom Rubisco shows greater variation in $K_C$ (23–68 μM), $S_{C/O}$ (57–116 mol mol$^{-1}$), and $K_O$ (413–2032 μM) relative to plant and algal Rubisco. The broad range of $K_C$ values mostly exceed those of $C_4$ plant Rubisco, suggesting that the strength of the carbon-concentrating mechanism (CCM) in diatoms is more diverse, and more effective than previously predicted. The measured $k_{cat}^c$ for each diatom Rubisco showed less variation (2.1–3.7 s$^{-1}$), thus averting the canonical trade-off typically observed between $K_C$ and $k_{cat}^c$ for plant Form I Rubisco. Uniquely, a negative relationship between $K_C$ and cellular Rubisco content was found, suggesting variation among diatom species in how they allocate their limited cellular resources between Rubisco synthesis and their CCM. The activation status of Rubisco in each diatom was low, indicating a requirement for Rubisco activase. This work highlights the need to better understand the correlative natural diversity between the Rubisco kinetics and CCM of diatoms and the underpinning mechanistic differences in catalytic chemistry among the Form I Rubisco superfamily.**

**Key words:** Algae, carbon fixation, diatoms, kinetics, photosynthesis, Rubisco.

## Introduction

Ribulose-1,5-bisphosphate carboxylase oxygenase (Rubisco) plays a fundamental role in photosynthetic $CO_2$ assimilation within the global carbon cycle. Rubisco activity within the terrestrial and ocean biospheres contributes approximately equally to the 10 Pmol of $CO_2$ annually fixed into organic carbon (Raven, 2009). Often the rate of $CO_2$ fixation is limited by Rubisco activity and, as such, has made the enzyme a primary target to enhance crop photosynthesis and yield through genetic manipulation (Mueller-Cajar and Whitney, 2008; Peterhansel *et al.*, 2008; Carmo-Silva *et al.*, 2015). However, improving Rubisco kinetics has proved difficult as a result of the complex assembly pathway of Rubisco in higher plants (Whitney *et al.*, 2011; Hauser *et al.*, 2015) and apparent trade-offs in its kinetic parameters (Tcherkez *et al.*, 2006;

Savir et al., 2010). Widening our understanding of the natural diversity in Rubisco is critical if solutions to improve its performance are to be found and understood (Parry et al., 2013). Of particular interest is Rubisco from organisms adapted to different environments. This includes marine phytoplankton whose efficient carbon-concentrating mechanisms (CCMs) enable them to endure, sometimes thrive in, nutrient- and $CO_2$-depleted seawater (Nelson et al., 1995).

In nature, Rubisco is found in a variety of oligomeric forms and within a diverse array of organisms that include archaea, photosynthetic bacteria, cyanobacteria, algae, and plants (Whitney et al., 2011). Form I Rubisco consists of eight large and eight small subunits, and is subdivided into Forms IA–ID depending on its sequence and lineage (Tabita et al., 2008). Most research to date on Rubisco has focused on those sourced from the terrestrial biosphere, with comparatively little characterization of Rubisco from oceanic sources. The terrestrial biosphere is dominated by the 'green' chloroplast lineage pertaining to plants and green algae that contain Form IB Rubisco (Tabita et al., 2008). However, oceanic photosynthesis is primarily carried out by phytoplankton containing chloroplasts from a 'red' lineage that comprise Form ID Rubisco (Delwiche and Palmer, 1997; Yoon et al., 2002; Falkowski et al., 2004). A group of phytoplankton called diatoms are of particular interest due to their importance in ocean primary productivity (estimated to account for ~20% of global primary production; Nelson et al., 1995), thus influencing global biogeochemical cycles, and for producing silicified walls that preserve paleoclimate signals in the fossil record (Armstrong et al., 2001; Egan et al., 2013; Heureux and Rickaby, 2015).

Compared with other photosynthetic enzymes, Rubisco is considered inefficient due to its low $CO_2$-saturated $CO_2$ fixation rate ($k_{cat}^c$) and low affinity for $CO_2$ (i.e. an elevated Michaelis constant, $K_m$, for $CO_2$; $K_C$). The basis of this inefficiency arises from the complex catalytic mechanism of Rubisco that imposes biochemical trade-offs between $k_{cat}^c$, $K_C$, and specificity for $CO_2$ over its competitive inhibition by $O_2$ ($S_{C/O}$) (Tcherkez et al., 2006). Recent analyses show that the extent of these trade-offs is variable between the Form I Rubisco of plants, red algae, and cyanobacteria (Tcherkez, 2013, 2015). Notably Rubisco oxygenation produces 2-phosphoglycolate, which is toxic to the chloroplast (Zelitch et al., 2009), necessitating its removal via the photorespiratory pathway at a cost of energy and fixed carbon (Peterhansel et al., 2008). The loss of $CO_2$ by photorespiration can be as high as 25% of the total carbon fixed in $C_3$ flowering plants (Laing et al., 1974).

Despite the catalytic inefficiencies of Rubisco, it appears that it can adapt to the $CO_2$:$O_2$ ratio of its environment. This is particularly evident for Rubisco kinetics in $C_3$ and $C_4$ plants. While $C_3$ plants rely on diffusion of $CO_2$ from the air to chloroplast stroma, $C_4$ plants utilize a CCM to elevate $CO_2$ around Rubisco to avoid photorespiration and its associated cellular resource costs. In response to higher intracellular $CO_2$, $C_4$ Rubisco has evolved improvements in $k_{cat}^c$ at the expense of reducing $CO_2$ affinity (i.e. increasing $K_C$) (Yeoh et al., 1980; Seemann et al., 1984; Ghannoum et al., 2005). The CCM and higher $k_{cat}^c$ allow $C_4$ plants to reduce their investment in Rubisco, lower the rate of photorespiration, and allow for carbon fixation rates similar to $C_3$ plants under low stomatal apertures (Sage, 2004; Ghannoum et al., 2005; Way et al., 2014). These features improve the nitrogen, energy, and water use efficiencies of $C_4$ plants.

In the oceans, the low levels of $CO_2$, and its slow diffusion rate in water, have led many photosynthetic organisms to evolve CCMs that utilize the higher concentrations of bicarbonate. These mechanisms are different from the CCMs of $C_4$ plants that arose during the low $CO_2$ concentrations of the Oligocene period (Sage, 2001; Osborne and Sack, 2012) and the coupled warmer, arid environments that trigger stomatal closure and N limitation of the soil (Ehleringer et al., 1997; Long, 1999). The $C_4$ plant CCM fixes $HCO_3^-$ by phosphoenolpyruvate (PEP) carboxylase, leading to production of $C_4$ organic acids in the Rubisco-lacking mesophyll cells. These $C_4$ organic acids then diffuse into the Rubisco-containing bundle sheath cells where they are decarboxylated (Sage, 2004). This process facilitates the concentration of $CO_2$ to levels that effectively saturate Rubisco (Furbank and Hatch, 1987).

While some diatoms may also have a $C_4$-like mechanism (Reinfelder et al., 2000, 2004) or a $C_3$–$C_4$ intermediate-like mechanism (Roberts et al., 2007), they contain a CCM suited to their single-celled physiology and high bicarbonate aquatic environment. In diatoms, the CCM consists of various bicarbonate transporters (Nakajima et al., 2013) and differing forms of carbonic anhydrase that serve to elevate $CO_2$ levels within the pyrenoid, a low $CO_2$-permeable subcellular compartment containing most of the cellular Rubisco (Reinfelder, 2010; Hopkinson et al., 2011). The efficiency of their CCMs allows diatoms to invest their scarce cellular resources conservatively in Rubisco. Accordingly the Rubisco content of diatoms is considerably lower [2–6% (w/w) of total cellular protein] than the 20–50% (w/w) Rubisco content of the soluble protein in plant leaves (Losh et al., 2013; Carmo-Silva et al., 2015).

Our understanding of phytoplankton CCM components and activity regulation remain rudimentary. This is despite the increasing interest in understanding how Form ID Rubisco and CCMs co-evolved and how carbon fixation rates by phytoplankton will respond to rising anthropogenic $CO_2$ (Raven et al., 2012; Young et al., 2012, 2013). From the few Form ID Rubisco kinetics determined, there is a strong signal of positive selection within the evolution of the Rubisco large subunits in red algae, Haptophytes, and diatoms (Young et al., 2012). Rubiscos from red algae have the highest specificities for $CO_2$ over $O_2$ ($S_{C/O}$; ~130–240 mol mol$^{-1}$) while the lower $S_{C/O}$ diatom Rubisco (~60–115 mol mol$^{-1}$) overlaps with the less diverse $S_{C/O}$ values of $C_3$ plant and $C_4$ plant Rubisco (~70–90 mol mol$^{-1}$) (Read and Tabita, 1994; Whitney et al., 2001, 2011; Haslam et al., 2005). $K_C$ measurements for diatom Rubisco (~28–40 µM, Badger et al., 1998; Whitney et al., 2001) exceed the concentration of $CO_2$ in the surface ocean (~13 µM in air-equilibrated surface seawater at 20 °C), exemplifying the requirement for a CCM. Modeling of the CCM in phytoplankton is highly reliant on measurements of their Rubisco kinetics (Hopkinson, 2011, 2014). However, the paucity of catalysis measurements for diatom Rubisco—and other phytoplankton—continue to limit reliable assessments of CCM function in microalgae.

In this study, we evaluate the diversity of Rubisco kinetics in 11 different diatom species at the common assay temperature of 25 °C. From measurements of $S_{C/O}$, $k_{cat}^{c}$, $K_C$, and the $K_m$ for $O_2$ ($K_O$), we determine the catalytic turnover rate for $O_2$ ($k_{cat}^{o}$) and unveil an unexpected large degree of kinetic variability across the species studied. Uncovered are novel relationships between kinetic parameters not previously observed for other plant and algal Form I Rubisco isoforms. Presented are a novel, robust data set of Rubisco kinetics in marine phytoplankton that provide new insight into potential constraints on microalgal photosynthesis that arise from variations in the effectiveness of their CCM to elevate $CO_2$ around Rubisco.

## Materials and methods

### *Species selection and sampling:*

Eleven species of marine diatoms were selected from cultures maintained at Princeton University and the Australian National University (ANU). Strains from Princeton University were grown at 20 °C under continuous light (~150 µmol photons $m^{-2}$ $s^{-1}$) in 0.2 µm filtered seawater supplemented with Aquil medium (Sunda *et al.*, 2005) and included the diatoms *Thalassiosira weissflogii* (CCMP 1336), *Skeletonema marinoi* (CCMP 1332), *Chaetoceros calcitrans* (CCMP 1315), *Chaetoceros muelleri* (CCMP 1316), and *Phaeodactylum tricornutum* (CCMP 642). *Fragilariopsis cylindrus* (CCMP 1102) was grown at 1 °C, 12:12 light:dark cycle at 75 µmol photons $m^{-2}$ $s^{-1}$. Strains from ANU were grown at 25 °C under a 16:8 light:dark cycle (~150 µmol photons $m^{-2}$ $s^{-1}$) cultured in 0.2 µm filtered seawater supplemented with F/2 medium and included the diatoms *Thalassiosisra oceanica* (CS-427), *Chaetoceros calcitrans* (CS-178), *Phaeodactylum tricornutum* (CS-29), *Bellerochea* sp. (CS-874/01), and *Cylindrotheca fusiformis* (CS-13).

### *Materials*

Unlabeled and $^{3}$H-labeled ribulose-1,5-bisphosphate (RuBP) was synthesized and purified as described (Kane *et al.*, 1998), and used to prepare $^{14}$C-labeled carboxypenitol-$P_2$ ([$^{14}$C]CPBP) according to Pierce *et al.* (1980) and Zhu and Jensen (1991).

### *Rubisco extraction*

Cells were harvested at or near exponential growth by gentle centrifugation (2000 *g* for 10 min) and the 0.1–0.5 ml cell pellets were snap-frozen in liquid nitrogen and stored at –80 °C. Pellets were re-suspended in 5 ml of ice-cold extraction buffer containing 50 mM EPPS-NaOH, pH 8.0, 1 mM EDTA, 2 mM DTT, and 1% (v/v) plant protease inhibitor cocktail (Sigma-Aldrich, St Louis, MO, USA), and cells were ruptured in a French press. Extract was centrifuged at 14 000 *g*, 4 °C for 2 min and the supernatant was used to quantify Rubisco $K_C$ *and* $k_{cat}^{c}$ or used to purify Rubisco and measure $CO_2/O_2$ specificity ($S_{C/O}$)

### *$CO_2/O_2$ specificity*

Rubisco was rapidly purified from ~1 g (~4–5 pooled biological replicates) of the –80 °C stored cells extracted in ice-cold extraction buffer, and lysed using a French press. Polyvinylpolypyrrolidone [1% (w/v)] was added to the lysate to remove secondary metabolites prior to centrifugation (17 600 *g*, 4 °C, 5 min). The soluble cellular protein was rapidly passed over a 1 ml Bio-Scale Mini Macro-Prep High Q ion exchange column (Biorad, Hercules, CA, USA) equilibrated with column buffer (50 mM EPPS-NaOH, pH 8.0, 1 mM EDTA). Bound Rubisco was eluted in 1.5 ml of column elution buffer (50 mM EPPS-NaOH, pH 8.0, 1mM EDTA 0.8 M NaCl) and concentrated to 0.5 ml using an Amicon Ultra-15 centrifugal filter (30 000 NMWL, Millipore, Billerica, MA, USA). The protein was applied to the Superdex 200 (GE Life Sciences) column to purify and desalt the Rubisco further. Fractions containing Rubisco were pooled and concentrated again by centrifugal filtration to 0.25 ml and glycerol was added to 20% (v/v) final concentration before freezing in liquid nitrogen and storing at –80 °C. Purified Rubisco preparations were used to measure $CO_2/O_2$ specificity using the method of Kane *et al.* (1994).

### *$K_C$, $k_{cat}^{c}$, $K_O$, and $k_{cat}^{o}$*

Rubisco content was quantified by [$^{14}$C]2-CABP (2-C-carboxyarabinitol 1,5-bisphosphate) binding as described by Sharwood *et al.* (2008) by incubating duplicate aliquots of soluble cellular protein extracts with 15 mM $NaHCO_3$, and 15 mM $MgCl_2$ and either 15 µM or 30 µM [$^{14}$C]CPBP for 10–30 min at 25 °C. The recovered amount of [$^{14}$C]CABP-bound Rubisco in both reactions varied by <2% ensuring the Rubisco catalytic site content was accurately quantified. RuBP-dependent $^{14}CO_2$ fixation assays were performed in 7 ml septum-capped scintillation vials at 25 °C as described (Whitney and Sharwood, 2007) using soluble diatom protein extract following 10–15 min activation with 15 mM $NaH^{14}CO_3$ and 15 mM $MgCl_2$. After activation, kinetic measurements were made on soluble cellular protein in assay vials containing reaction buffer (0.5 ml of 100 mM EPPS-NaOH, pH 8, 15 mM $MgCl_2$, 0.6 mM ribulose-$P_2$, 0.1 mg $ml^{-1}$ carbonic anhydrase) equilibrated with 0, 21, 40, and 60% (v/v) $O_2$ in $N_2$ and five differing concentrations of $^{14}CO_2$ (between 10 µM and 100 µM; specific activities of ~1800 cpm $nmol^{-1}$ $CO_2$ fixed). The assays were stopped after 1–3 min with 0.5 vols of 25% (v/v) formic acid and processed for scintillation counting. Values for $K_C$ and maximal carboxylase activity ($v_c^{max}$) were extrapolated from the data using the Michaelis–Menten equation as described by Sharwood *et al.* (2008) and Whitney *et al.*, (2011). Measures of $k_{cat}^{c}$ were calculated by dividing $v_c^{max}$ by the number of Rubisco active sites as determined by [$^{14}$C]2-CABP binding. $K_O$ was determined from the slope of the linear increase in $K_C$ in response to $O_2$. Values for $k_{cat}^{o}$ were calculated using the equation $k_{cat}^{o}=(k_{cat}^{c}\times K_O)/(K_C\times S_{C/O})$. All measurements were made in triplicate using material pooled from 2–3 biological replicates.

### *Statistics*

One-way ANOVA was performed to determine whether significant differences ($P$-value ≤0.05) existed between the Rubisco kinetics parameters measured in the different groups in Fig. 2. Where significant differences were found, Tukey's HSD tests were performed to determine which groups differed from each other. Linear regression was fit by least-square analysis, and the correlation coefficient ($r^2$) was based on standard error of estimate. Analysis of covariance (ANCOVA) was used to determine whether the linear fit was significant to 95% ($P$-value ≤0.05) in Table 2 and Figs 3 and 4.

## Results

Our results for 11 species of diatoms represent the largest data set of Form ID Rubisco kinetics available to date. The diatom species selected in this study represent a wide range of habitats and evolutionary diversity (Table 1), and included multiple strains of the same species (*P. tricornutum* and *C. calcitrans*), and one polar pennate (*F. cylindrus*).

### *Rubisco activation and stability in diatom cellular protein extract*

The maintained stability of Rubisco activity in isolated soluble leaf protein facilitates the accurate and reliable measure of maximum carboxylation rates ($k_{cat}^{c}$) and the

**Table 1.** *Diatom strains, location of isolation, and Rubisco kinetics measured at 25 °C*

| Species | Location isolated | $k_{cat}^c$ ($s^{-1}$) | $K_C$ (μM) | $k_{cat}^o$ ($s^{-1}$) | $K_O$ (μM) | $S_{C/O}$ (mol $mol^{-1}$) | $K_C^{21\%O2}$ (μM) | $k_{cat}^c/K_C$ (mM $s^{-1}$) | $k_{cat}^c/K_C^{21\%O2}$ (mM $s^{-1}$) |
|---|---|---|---|---|---|---|---|---|---|
| **Diatoms (Bacillariophyta)** | | | | | | | | | |
| *Thalassiosira weissflogii* (CCMP 1336)[a] | Gardiners Island, Long Island, NY, USA | 3.2±0.2 | 65±3 | 1.3 | 2032±458 | 79±1 | 73 | 49 | 44 |
| *Thalassiosira oceania* (CS-427)[a] | Little Swan port, Tasmania, Australia | 2.4±0.4 | 65±5 | 0.4 | 954±228 | 80±2 | 83 | 36 | 28 |
| *Skeletonema marinoi* (CCMP 1332)[a] | Milford, CT, USA | 3.2±1.1 | 68±8 | ND | 883±346 | ND | 88 | 47 | 36 |
| *Chaetoceros calcitrans* (CCMP 1315) | Collection site unknown | 2.6±0.2 | 25±1 | 0.8 | 413±53 | 57±11 | 41 | 103 | 64 |
| *Chaetoceros muelleri* (CCMP 1316) | Oceanic Institute, HI, USA | 2.4±0.3 | 23±1.5 | 0.5 | 425±67 | 96±2 | 37 | 104 | 65 |
| *Chaetoceros calcitrans* (CS-178) | Unknown (but should be synonymous with CCMP 1315) | 3.4±0.6 | 31±2 | 0.7 | 490±54 | 75±1 | 47 | 112 | 74 |
| *Bellerochea cf. horologicalis* (CS-874/01) | Ilbilbie, Queensland, Australia | 2.1±0.2 | 50±4 | ND | 764±190 | ND | 67 | 41 | 31 |
| *Phaeodactylum tricornutum* (UTEX 642) | Plymouth, UK | 3.2±0.9 | 36±1 | 0.5 | 592±44 | 108±2 | 52 | 88 | 62 |
| *Phaeodactylum tricornutum* (CS-29) | Unknown, UK | 3.3±0.6 | 41±1 | 0.5 | 664±54 | 116±2 | 57 | 81 | 59 |
| *Fragilariopsis cylindrus* (CCMP 1102) | Islas Orcadas Cruise, Station 12 | 3.5±0.3 | 64±8 | 0.5 | 667±255 | 77±1 | 88 | 55 | 40 |
| *Cylindrotheca fusiformis* (CS-13) | Halifax, Canada | 3.7±0.2 | ND | ND | ND | 79±1 | ND | ND | ND |
| **Higher plants (controls)** | | | | | | | | | |
| *Nicotiana tabacum* (tobacco, $C_3$) | | 3.1±0.3 | 9.7±0.1 | 1.1 | 283±15 | 82±1 | 18.3 | 316 | 167 |
| *Zea mays* (maize, $C_4$) | | 5.5±0.2 | 19.0±0.6 | 1.4 | 397±59 | 88±2 | 31 | 289 | 177 |

[a] Belonging to the order Thalassiosirales;
Values shown are average of measurements from $n \geq 3$ (± SD) biological repeat samples (see figure legends); ND, not determined
$K_C^{21\%O2}$ was calculated as $K_C(1+O_2/K_O)$ assuming air-saturated $O_2$ levels in $H_2O$ of 252 μM

Michaelis–Menten (half-saturation) constant ($K_m$) for carboxylation ($K_C$) without need of a purification step (Sharwood *et al.*, 2008). These measurements require all eight catalytic sites in each $L_8S_8$ Rubisco molecule to be primed with $CO_2$-$Mg^{2+}$ (i.e. activated). *In vivo*, full activity is prevented by inhibitory binding of sugar phosphate molecules to the catalytic site (Andralojc *et al.*, 2012). In illuminated leaves, the ~4:1 molar ratio of RuBP:catalytic sites leads to RuBP binding to non-activated catalytic sites being the almost exclusive cause of inactivation (Price *et al.*, 1995). Upon cellular protein extraction, the levels of available RuBP deteriorate, facilitating RuBP dissociation (and fixation) and catalytic site activation. As shown in Fig. 1A (time zero), Rubisco from newly expanded upper canopy tobacco leaves is ~80% activated *in vivo.* At 25 °C, full activation (i.e. dissociation of all inhibitory RuBP) of tobacco Rubisco in all three leaf samples tested occurred within ~5 min *in vitro* and full activity was maintained over the 20 min test period.

In contrast to the control tobacco Rubisco *in vitro* activation assays, the activation status of Rubisco in each phytoplankton species was lower, varying between ~20% (*Thalassiosira oceania*, *T. weissflogii*, *Cylindrotheca fusiformis*, and *Phaeodactylum tricornutum*) to ~70% (*Skeletonema ardens*). Accordingly, longer incubation times at 25 °C were required to activate their Rubisco fully *in vitro* (Fig. 1B–H). Nevertheless, in all phytoplankton samples, Rubisco was fully activated within 10 min of extraction at 25 °C and the activity was stable for at least a further 10 min.

### *Rubisco kinetics are highly variable both between and within diatom species.*

Measurements of $k_{cat}^c$, $K_C$, maximum oxygenation rates ($k_{cat}^o$), $K_m$ for $O_2$ ($K_O$), and the specificity for carboxylase over oxygenase ($S_{C/O}$) were measured at 25 °C to allow for direct comparison with other Rubisco kinetics in the literature. As shown in Table 1, there is significant variation in diatom Rubisco catalysis, with differences even found between Rubisco from the same genus (*Chaetoceros*). Also included in these analyses were control catalysis measurements for Rubisco from tobacco ($C_3$ plant) and maize ($C_4$ plant) whose values match those previously measured (Supplementary Table S1 at *JXB* online). In the following, we compare our results with kinetics measured at 25 °C for other Form ID Rubiscos from red algae and Form IB Rubisco from $C_3$ and $C_4$ plants (taken from Badger *et al.*, 1998; Savir *et al.*, 2010).

Among the diatom Rubiscos analyzed, there was a <2-fold variation in $k_{cat}^c$, which ranged from $2.1 \pm 0.2\ s^{-1}$ in *Bellerochea* cf. *horologicalis* to $3.7 \pm 0.2\ s^{-1}$ in *C. fusiformis*. As shown in Fig. 2A, $k_{cat}^c$ varied significantly between the groups (one-way ANOVA, $F$=25.1, $P$<0.001). Further testing with Tukey HSD showed that diatom $k_{cat}^c$ values were comparable with those of Rubisco from $C_3$ plants but statistically lower than those from $C_4$ plants ($P$<0.01) and higher than those from red algae ($P$<0.01). Diatom Rubisco also showed diversity in the oxygenation rates (Fig. 2B). The measured $k_{cat}^o$ values of $0.4–1.6\ s^{-1}$ were significantly lower than those of $C_3$ plants, but not lower than those of $C_4$ plants or red algae (one-way

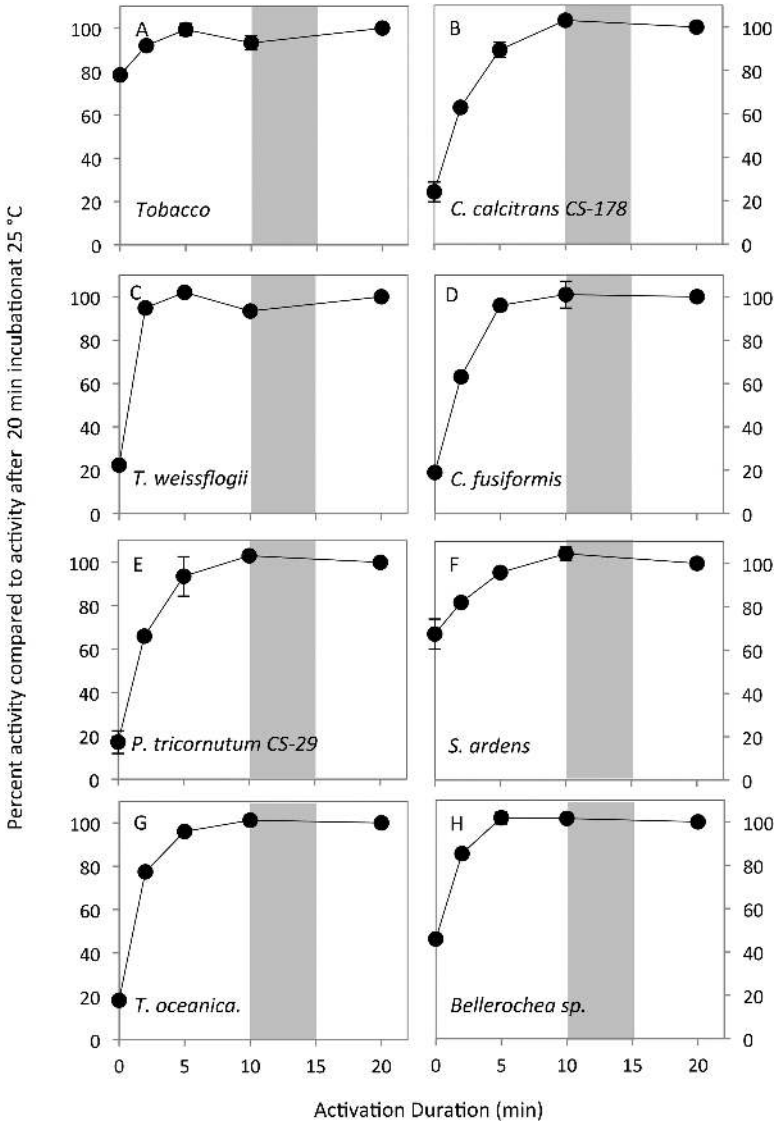


**Fig. 1.** Measurement of Rubisco activation status, maximal activity, and stability *in vitro* at 25 °C. Soluble cellular protein rapidly extracted from tobacco and each phytoplankton in $CO_2$-free extraction buffer (containing 5 mM $MgCl_2$) was used to measure changes in the Rubisco $^{14}CO_2$ fixation rate after activating the extract for 0–20 min in buffer containing 15 mM $MgCl_2$ and 15 mM $NaHCO_3$. Gray shading indicates the time when protein extract was assayed to quantify $k_{cat}^c$, $K_C$, and $K_O$ (Table 1). Data represent measures from duplicate biological samples (± SD).

ANOVA, $F$=5.25, $P$=0.008, Tukey HSD between diatoms and $C_3$ plants $P$=0.007).

With regard to $CO_2$ affinity, the $K_C$ values of diatom Rubisco varied >2.7 fold (25–68 µM; Fig. 2C) and were significantly higher than those of Rubisco from red algae, and $C_3$ and $C_4$ plants (one-way ANOVA, $F$=19.5, $P$<0.001, Tukey HSD $P$<0.01 for all three pairs). Only cyanobacteria have a lower $CO_2$ affinitty than diatoms, with $K_C$ values in the range 200–260 µM, which accords with the effectiveness of their CCM (Price *et al.*, 2008; Whitney *et al.*, 2011; Hopkinson *et al.*, 2014). In contrast, diatom Rubisco $K_O$ values were not statistically different from those of red algae, $C_3$, or $C_4$ plants (one-way ANOVA, $F$=1.44, $P$=0.26). Of particular interest was the low $O_2$ affinity of *T. weissflogii* Rubisco whose $K_O$ exceeded 2 mM $O_2$.

Improving the $S_{C/O}$ of Rubisco, without unfavorably changing its other kinetic parameters, is a prized goal as it has a pervasive influence on Rubisco efficiency in organisms both with and without CCMs (Long *et al.*, 2015). While the $S_{C/O}$ range in $C_3$ and $C_4$ plants shows limited diversity, a 2-fold variation was found in the $S_{C/O}$ of diatom Rubisco at 25 °C (i.e. 57–116 mol mol$^{-1}$; Table 1) and encompassed the range found previously in diatoms (Badger *et al.*, 1998; Whitney *et al.*, 2001; Haslam *et al.*, 2005). Despite this large variation, the $S_{C/O}$ of diatom Rubisco was not significantly different from that of $C_3$ and $C_4$ plants, and failed to reach the high $S_{C/O}$ of Rubisco from red algae (Fig. 2E). In terms of carboxylation efficiency ($k_{cat}^c/K_C$), we find that diatom Rubisco is low compared with red algae, and $C_3$ and $C_4$ plants (one-way ANOVA, $F$=11.5, $P$=0.0002, Fig. 2F, Tukey HSD $P$=0.04, $P$=0.001, and $P$=0.005, respectively), even in the presence of ambient $O_2$ levels (i.e. $k_{cat}^c/K_C^{21\%O2}$; Table 1).

### *Novel kinetic relationships of diatom Rubisco*

A number of trade-offs between Rubisco kinetic parameters have been observed across a range of primary producers

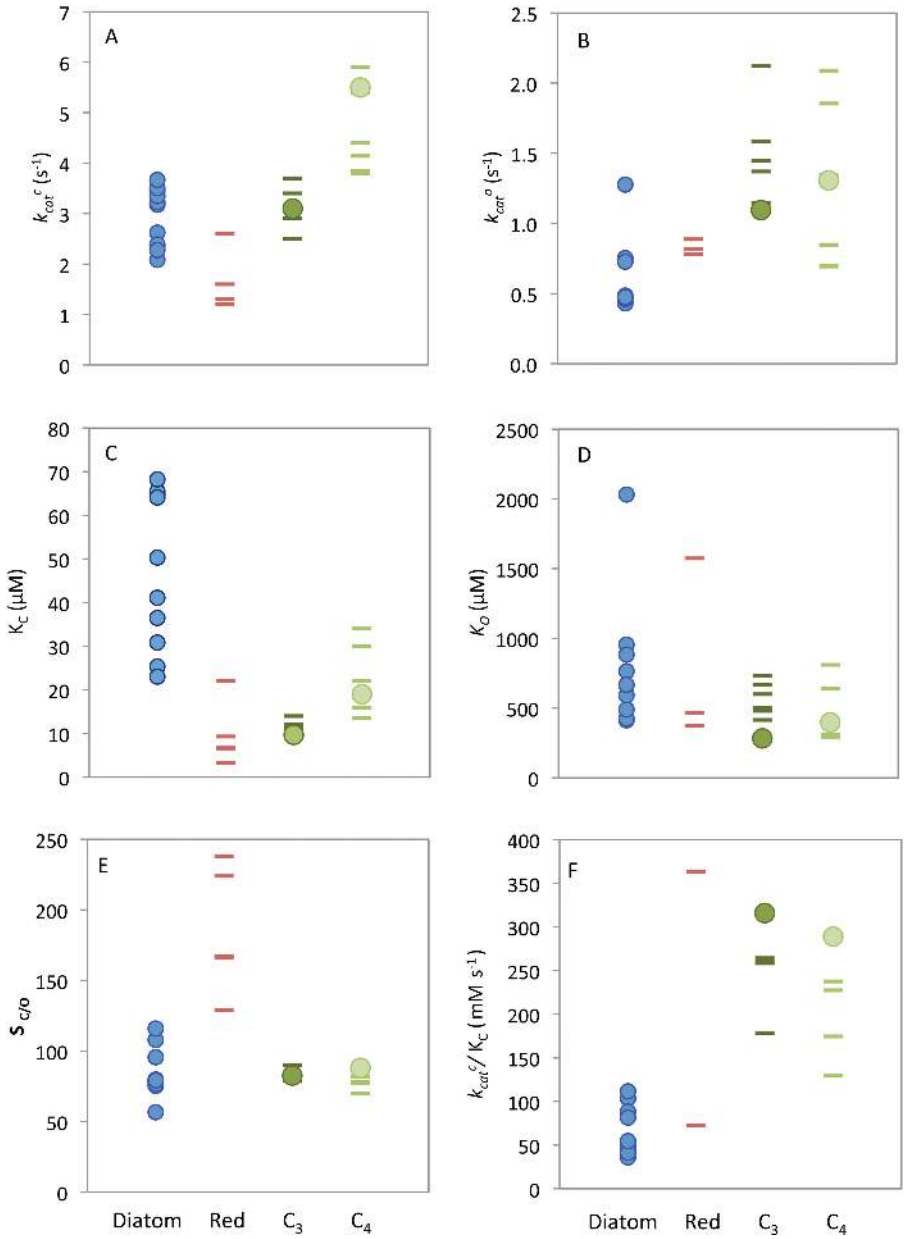


**Fig. 2.** Rubisco kinetic parameters measured at 25 °C. Rubisco properties measured from diatoms (blue circles), tobacco and maize (green circles, see Table 1) compared with previously published values for red algae (red, maroon dashes), $C_3$ plants (dark green dashes), and $C_4$ plants (light green dashes) (Badger *et al.*, 1998; Savir *et al.*, 2010; Supplementary Table S1). Kinetic parameters include (A) the maximum rates of carboxylation ($k_{cat}^{c}$), (B) oxygenation rate ($k_{cat}^{o}$), the $K_m$ for (C) $CO_2$ ($K_C$) and (D) $O_2$ ($K_O$), (E) the specificity for $CO_2$ over $O_2$ ($S_{C/O}$), and (F) the carboxylation efficiency ($k_{cat}^{c}/K_C$, mM $s^{-1}$).

(Tcherkez *et al.*, 2006; Savir *et al.*, 2010). From the relatively small data set examined, relationships between the varied Rubisco kinetic parameters (i.e. $K_C$, $k_{cat}^{c}$, $k_{cat}^{o}$, $S_{C/O}$, and $K_O$) appear confined to a one-dimensional landscape, with simple power law correlations between parameters (Savir *et al.*, 2010). We examined these relationships by comparing the kinetic parameters of diatom Rubisco with those measured in green algae, red algae, and plants using data sets of Tcherkez *et al.* (2006), Savir *et al.* (2010), Whitney *et al.* (2011), and Galmes *et al.* (2014) (see Supplementary Table S1).

As shown recently by Tcherkez (2015), the well-documented trade-off between $K_C$ and $k_{cat}^{c}$ varies between organisms. For plant and algal Form I Rubisco, the correlation between $K_C$ and $k_{cat}^{c}$ varies from that seen for Form I Rubisco from cyanobacteria and other prokaryotes (Tcherkez, 2013). With regard to eukaryotic Form I Rubisco, the diatom variants uniquely show no correlation between $K_C$ and $k_{cat}^{c}$ (Fig. 3A). The linear correlation of $r^2$=0.36, $P$=1.1×10$^{-6}$ between $k_{cat}^{c}$ versus $K_C$ for plant and eukaryotic algal Form I Rubisco (Fig. 3A, gray circles), became insignificant when diatom data were included (Fig. 3A, black circles, $r^2$=0.013, $P$=0.36). This suggests that the catalytic mechanism of diatom Rubisco may differ relative to other eukaryotic variants—possibly through changes to one or more of the elemental steps in the Rubisco catalytic cycle.

A positive linear correlation between $K_C$ and $K_O$ was found among diatom Rubisco ($r^2$=0.43, $P$=0.041; Fig 3B) that was strengthened when the outlying high $K_O$ value (i.e. low $O_2$ affinity) for *T. weissflogii* Rubisco was removed ($r^2$=0.83, $P=5.8\times10^{-4}$). Form 1 Rubisco from other plants and eukaryotic algae also displays a significant positive correlation ($r^2$=0.24, $P=3.73\times10^{-4}$), and the strength of this relationship increases ($r$=0.41, $P=5.0\times10^{-8}$) when the diatom measurements are included.

Diatom Rubiscos also showed no statistically significant relationship between carboxylase efficiencies and $S_{C/O}$ ($r^2$<0.002, $P$=0.5; Fig 3C). Although diatom carboxylation efficiencies are lower than those of higher plant Rubisco (Fig 2F), the diatom $S_{C/O}$ values are within a similar range, indicating that oxygenase efficiencies must also be correspondingly lower than those of plants, probably due to the lower $k_{cat}^{o}$ rates of diatom Rubisco (Fig 2B).

While a weak positive relationship between $k_{cat}^{o}$ and $K_O$ has been shown by Tcherkez (2015), we found that such a correlation did not extend to diatom Rubisco ($r^2$=0.38, $P$ =0.078) (Fig. 3D, black circles) or when combined with plant and other eukaryotic algal Rubisco (Fig. 3D, gray circles). In addition, no relationship between $k_{cat}^{c}$ and either $K_C/K_O$ or $S_{C/O}$ was evident in the diatom Rubisco data set, although for these comparisons our values fall within the noise of the data analyzed by Savir *et al.* (2010). Linear regressions were tested between all kinetic parameters of diatom Rubiscos and are shown in Table 2.

### *Rubisco carboxylation efficiency versus Rubisco content*

Compared with $C_3$ plants, the faster carboxylation rates of Rubisco in $C_4$ plants enable them to invest less of their N resources in Rubisco (Seemann *et al.*, 1984; Ghannoum *et al.*, 2005). We therefore compared the Rubisco content measured in a range of diatoms and the Haptophyte *Isochrysis galbana* in exponentially growing cells (same strains grown under the same conditions; see Losh *et al.*, 2013) against our measured values of $k_{cat}^{c}$ and $K_C$ (Table 1). We found no relationship between Rubisco content and $k_{cat}^{c}$, but observed a positive correlation between Rubisco content and carboxylation efficiency in the presence of 21% $O_2$ ($k_{cat}^{c}/K_C^{21\%O2}$), which is driven by the negative correlation of Rubisco content with $K_C^{21\%O2}$ (Fig. 4). These relationships are also apparent when Rubisco content is plotted against carboxylation efficiency and $K_C$ in the absence of $O_2$, but with a lower correlation coefficient.

## Discussion

In this study, we demonstrate the large catalytic diversity of Rubisco among 11 diatom species. A unique property of diatom Rubisco is that it lacks the relationship between $CO_2$-fixing speed ($k_{cat}^{c}$) and $CO_2$ affinity ($K_C$) shared by many higher plant and algal Form I Rubisco isoforms. Our

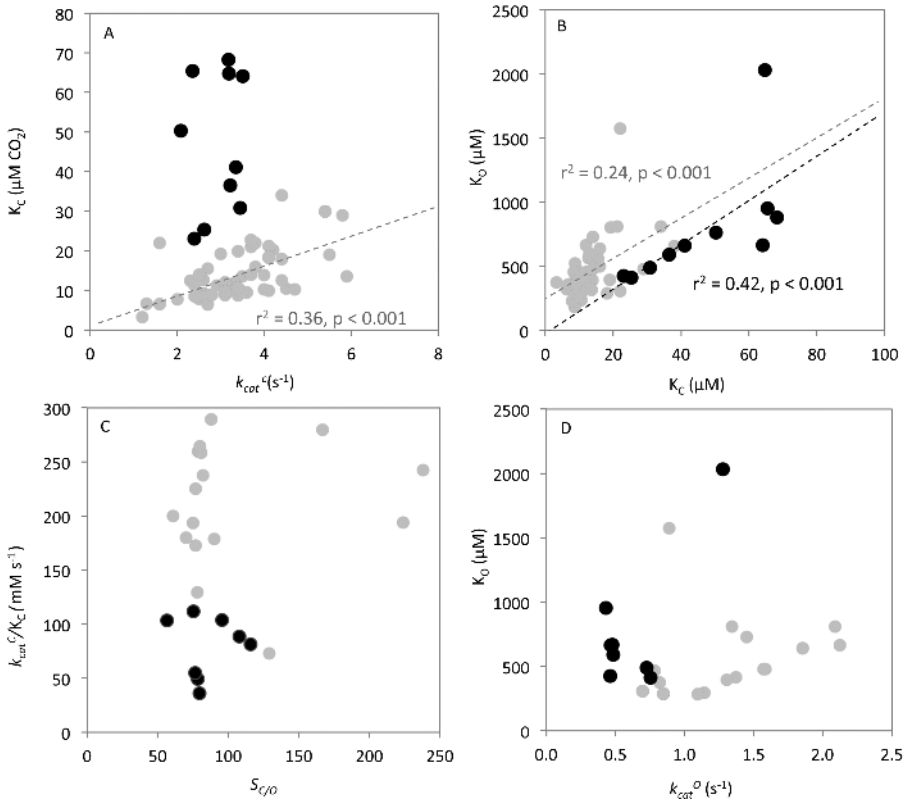


**Fig. 3.** Comparing the catalytic relationships of diatom and other Form I Rubiscos. Comparison of (A) maximum carboxylation rate ($k_{cat}^{c}$) versus the $K_m$ for $CO_2$ ($K_C$), (B) $K_C$ versus the $K_m$ for $O_2$ ($K_O$), (C) the carboxylation efficiency ($k_{cat}^{c}/K_C$) versus specificity for $CO_2$ over $O_2$ ($S_{C/O}$), and (D) the maximum oxygenation rate ($k_{cat}^{o}$) and $K_O$. Measured for diatoms (black circles) and compared with the compilation of plants and eukaryotic algae from Savir *et al.* (2010), Badger *et al.* (1998), Whitney *et al.* (2011), and Galmes *et al.* (2014) (gray circles).

**Table 2.** *Linear correlations between various Rubisco kinetic parameters from 11 diatom species*

| | $k_{cat}^{c}$ | $K_C$ | $K_O$ [a] | $S_{C/O}$ | $k_{cat}^{o}$ | $k_{cat}^{c}/K_C$ | $k_{cat}^{o}/K_O$ | $K_C/K_O$ | $K_C^{21\%O2}$ | $k_{cat}^{c}/K_C^{21\%O2}$ |
|---|---|---|---|---|---|---|---|---|---|---|
| $k_{cat}^{c}$ | 1 | 0.0212 (0.688) | 0.0133 (0.752) | 0.0182 (0.729) | 0.0503 (0.562) | 0.0388 (0.585) | 0.0016 (0.919) | 0.0299 (0.633) | 0.0293 (0.637) | 0.103 (0.365) |
| $K_C$ | | 1 | **0.425 (0.0412)** | 0.00965 (0.817) | 0.181 (0.254) | **0.854 (0.000131)** | 0.223 (0.199) | 0.0715 (0.455) | **0.958 (<0.00001)** | **0.760 (0.00102)** |
| $K_O$ [a] | | | 1 | 0.00818 (0.831) | 0.378 (0.0783) | 0.350 (0.0714) | 0.209 (0.216) | 0.275 (0.120) | 0.240 (0.150) | 0.217 (0.175) |
| $S_{C/O}$ | | | | 1 | 0.178 (0.298) | 0.00189 (0.919) | **0.260 (0.196)** | 0.00782 (0.835) | 0.0126 (0.791) | 0.00195 (0.742) |
| $k_{cat}^{o}$ | | | | | 1 | 0.107 (0.390) | 0.125 (0.351) | 0.0914 (0.429) | 0.108 (0.389) | 0.0667 (0.502) |
| $k_{cat}^{c}/K_C$ | | | | | | 1 | 0.304 (0.124) | 0.0425 (0.568) | **0.803 (0.000448)** | **0.963 (<0.00001)** |
| $k_{cat}^{o}/K_O$ | | | | | | | 1 | 0.00552 (0.849) | 0.176 (0.260) | 0.228 (0.194) |
| $K_C/K_O$ | | | | | | | | 1 | 0.210 (0.183) | 0.0888 (0.403) |
| $K_C$ air | | | | | | | | | 1 | **0.752 (0.0116)** |
| $k_{cat}^{c}/K_C$ air | | | | | | | | | | 1 |

Correlation coefficient and probability of linear correlation, $r^2$ ($P$-value).
Relationships with statistically significant linear correlation ($P<0.05$) are shown in bold.
[a] Correlation when all data are included. This is different from the correlation shown in Fig. 2, which does not include the T. *weissflogii* outlier.

measured $K_C$ values for diatom Rubisco show larger diversity than observed in contemporary plant Form I Rubisco and, as a result, would require different $CO_2$ concentrations to saturate Rubisco. Our data suggest that the current estimates of $CO_2$ concentrations at the site of Rubisco in diatoms are significantly underestimated for some species. In addition, there is an unexpected negative relationship between $K_C^{21\%O2}$ and the Rubisco content in diatoms that suggests a trade-off in the allocation of resources (energy and nutrients) between investing in Rubisco production to sustain rates of photosynthesis for competitive growth or enhancing CCM capacity to sustain saturating $CO_2$ levels for Rubisco function.

### *No significant relationship exists between $k_{cat}^{c}$ and $K_C$*

A positive relationship between $k_{cat}^{c}$ and $K_C$ has been found in all Rubiscos studied to date, although there are increasing indications from wider surveys of Rubisco kinetics (Galmes *et al.*, 2014) that the relationship shared by plant and algal Rubisco differs from that observed for prokaryotic Form I Rubisco (Tcherkez, 2013, 2015). Remarkably, diatom Rubiscos in this study show no relationship between $K_C$ and $k_{cat}^{c}$, whereby their $C_3$ plant-like $k_{cat}^{c}$ values (Fig. 2A) contrast with atypically high $K_C$ values that generally exceed those of $C_4$ plant Rubisco (Fig. 2C). The lack of relationship is surprising as the trade-off between $K_C$ and $k_{cat}^{c}$ is thought to be due to a fundamental mechanistic constraint of their inter-related rate constants (Tcherkez *et al.*, 2006, 2012). However, differences in the relationships of $k_{cat}^{c}$ and $K_C$ between different photosynthetic groups may arise from differences in the intrinsic equilibrium of the RuBP enolization reaction (Tcherkez, 2013, 2015). More study is needed into the enolization, $CO_2/O_2$ addition, hydration, and cleavage reactions of Rubisco from diatoms (and other microalgae) to understand fully the extent and mechanistic foundation for the contrasting relationships between $k_{cat}^{c}$ and $K_C$ found in nature.

### *High $K_C$ values require higher concentrations of $CO_2$ to saturate*

Diatom Rubisco $K_C$ values are significantly higher than the concentration of $CO_2$ in seawater (~10 μM at 25 °C). Like $C_4$ plants, cyanobacteria, and many other photosynthetic organisms, diatoms are rarely limited by $CO_2$ for growth because they possess a CCM. The CCM varies between species, but all combine both morphological (such as the pyrenoid, carboxysome, and bundle sheath in diatoms, cyanobacteria, and $C_4$ plants, respectively) and biochemical (e.g. carbonic anhydrases and bicarbonate transporters) specialization to provide high $CO_2$ concentrations around the site of Rubisco. In $C_4$ plants, $CO_2$ concentrations within the bundle sheath chloroplasts are in excess of 160 μM (i.e. >5000 μbar; Furbank and Hatch, 1987) relative to the subsaturating $CO_2$ concentrations in $C_3$ chloroplasts (<10 μM). Similarly, the CCM of cyanobacteria provides highly saturating $CO_2$ levels of >400 μM within the carboxysome for their Rubisco (assuming a pH of 7.35 and a 15 mM inorganic carbon pool; Hopkinson *et al.*, 2014; Whitehead *et al.*, 2014).

Experimental determination of concentrations of $CO_2$ and $O_2$ in pyrenoids of diatoms is currently impossible. This

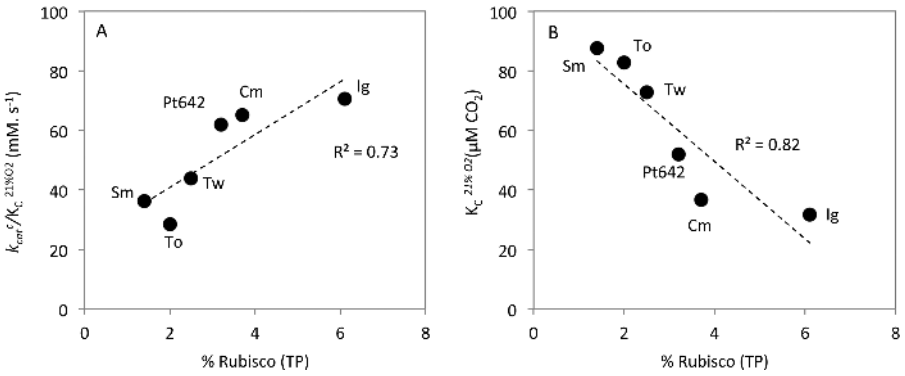


**Fig. 4.** Relationships of Rubisco content to catalysis. (A) Rubisco content as a percentage of total cellular protein (% TP) is positively correlated with carboxylation efficiency in 21% $O_2$ ($k_{cat}^c/K_C^{21\%O2}$). (B) This is largely driven by the negative correlation of Rubisco content with $K_C^{21\%O2}$. Rubisco content was taken from Losh *et al.* (2013). *I. galbana* (Ig), *C. muelleri* (Cm), *P. tricornutum* 642 (Pt642), *T. weissflogii* (Tw), *T. oceanica* (To), and *S. marinoi* (Sm).

has necessitated $CO_2$ levels being modeled according to conceptual understanding of the diatom CCM and its Rubisco kinetics. Based on a $K_C^{21\%O2}$ of ~41 μM for *P. tricornutum* Rubisco (Whitney *et al.*, 2001), a pyrenoid $CO_2$ concentration of ~110 μM was modeled (Hopkinson, 2014). While only 9-fold higher than surface seawater $CO_2$ concentrations, this $CO_2$ level would give ~75% saturation of Rubisco carboxylase activity. As shown in Table 1, this assumed $K_C^{21\%O2}$ value is at the lower end of the values measured in our study, indicating that most diatom species would require higher concentrations of $CO_2$ in the pyrenoid to attain similar saturation. For example, from our measures of $K_C^{21\%O2}$ (37–88 μM) the pyrenoid $CO_2$ concentrations would need to range between ~148 μM and 352 μM for 80% saturation (or ~92–272 μM in the absence of $O_2$). This adjustment would suggest that $CO_2$ concentrations in the pyrenoid are similar to, and possibly exceed, those measured in $C_4$ plant bundle sheath cells; see above and Furbank and Hatch (1987).

### *Energetic investment in the CCM and Rubisco*

The single-cell physiology of phytoplankton and variable nutrient availability of marine ecosystems require their expedient use and probably restricts the energy and resources that can be expended on photosynthesis. The investment of cellular resources in Rubisco synthesis is probably limited to the minimum concentration required for growth (Losh *et al.*, 2013) albeit in balance with the requirements of other cellular processes, such as the high energy costs of a CCM. Notably the resource investment by diatoms in Rubisco [e.g. 2–6% (w/w) of cellular protein; Fig. 3] is much smaller than that in the leaf soluble protein of $C_3$ plants [25–50% (w/w)] and $C_4$ plants [10–40% (w/w)] where it accounts for 5–25% of leaf N (Ghannoum *et al.*, 2005; Carmo-Silva *et al.*, 2015). The energy cost of a CCM depends on the capacity of phytoplankton to actively take up inorganic carbon at a rate that is proportional to the diffusive loss of $CO_2$ from the cell, which is influenced by the internal:external $CO_2$ gradient and the permeability of the pyrenoid to $CO_2$ (Hopkinson *et al.*, 2011; Raven *et al.*, 2014; Raven and Beardall, 2016). Diatoms appear well adapted to maintaining near-saturating $CO_2$ levels around Rubisco (Tortell *et al.*, 2000; Rost *et al.*, 2003; Chen and Gao, 2004; Kranz *et al.*, 2015) by regulating CCM activity in response to varying extracellular $CO_2$ (Chen and Gao, 2004; Hennon *et al.*, 2015; Young *et al.*, 2015). This 'energy minimization' strategy in CCM regulation and Rubisco production probably provides an N minimization strategy and a significant growth advantage to diatoms (Giordano *et al.*, 2005; Raven *et al.*, 2011).

Our study provides evidence for linkages between Rubisco $CO_2$ affinity and the efficiency of the CCMs in diatoms. Unlike in $C_4$ plants where improvements in $k_{cat}^c$ correlate with reduced N investment in Rubisco (Ghannoum *et al.*, 2005), diatom Rubisco content was positively correlated with carboxylation efficiency (Fig. 4A) not $k_{cat}^c$. This correlation was governed primarily by the strong negative relationship between Rubisco content and $K_C$ (both with and without 21% $O_2$; Fig. 4B). This leads us to hypothesize that diatoms balance resource allocation for photosynthesis between Rubisco content or the CCM. Diatoms such as *Thalassiosira* and *Skeletonema* species maintain low Rubisco content but require more resource allocation to their CCM to saturate their low-$CO_2$ affinity (high $K_C$) Rubiscos. Alternatively, diatoms such as *Phaeodactylum* and *Chaetoceros* species have higher Rubisco content and lower $K_C$ values, requiring lower $CO_2$ concentrations for saturation of carboxylation (Fig. 4). As summarized in Fig. 5, this hypothesis infers an evolutionary trade-off between Rubisco kinetics and content in diatoms; that is, the level of energy invested by diatoms in their CCM to attain $CO_2$ concentrations suited to their Rubisco $CO_2$ affinity, not its $k_{cat}^c$, influences resource availability for cellular metabolism, that includes Rubisco synthesis.

### *Co-evolution of Rubisco and CCMs*

Variations in the mechanistic chemistry of diatom Rubisco and plasticity in CCM efficiency among diatom species may explain the non-canonical kinetic features identified for diatom Rubisco (Fig. 3). Although the common ancestor of diatoms was thought to have gained a chloroplast from secondary endosymbiosis of a red alga ~1.2 billion years ago (Yoon *et al.*, 2002), diatoms only began to appear in the fossil record ~200 million years ago (Brown and Sorhannus, 2010). When, or how, the subsequent falling $CO_2$:$O_2$ levels triggered the evolution of

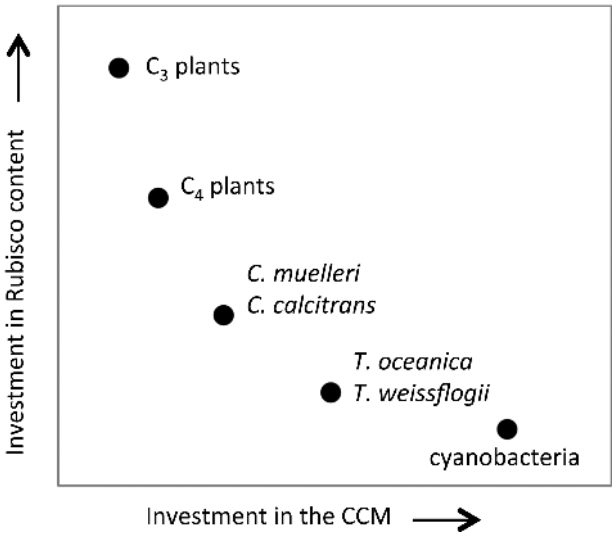


**Fig. 5.** Resource allocation hypothesis for the balance between Rubisco content and $K_C$ values. Organisms that invest their energy resources heavily in the CCM (e.g. cyanobacteria) to maintain high intracellular $CO_2$ levels to saturate Rubisco and limit photorespiration are able to reduce their resource investment in Rubisco. At the other end of the spectrum, organisms without a CCM (e.g. $C_3$ plants) have Rubisco that is undersaturated with $CO_2$ and require large resource investments in Rubisco content to maintain adequate rates of carbon fixation for survival. Organisms with a CCM fall somewhere along the saturation curve, depending on the carboxylation speed of their Rubisco and their potential to balance the investment of resources in Rubisco biogenesis suitably or maintain elevated intercellular $CO_2$ levels around Rubisco.

marine CCMs remains uncertain (Raven *et al.*, 2012). Notably, although sharing similar Form ID Rubiscos, the $S_{C/O}$ and carboxylation efficiencies of red algae are much higher than those of diatoms and, in some cases, those of higher plants (Whitney *et al.*, 2001). Comparative analyses of the large subunit for a small number of Form ID Rubiscos showed a clear signal of positive selection both between and within the major algal groups (Young *et al.*, 2012). In particular, positive selection was detected along the basal branch leading to diatoms, including between the centric diatom Thalassiosirales and Chaetocerales species, which accords with the very different $K_C$ values we observed in this study. Further work is needed to understand adaptation of Form ID Rubisco and to elucidate the amino acid changes in the large and/or small subunits responsible for the wide range of kinetic parameters observed in this study.

### *A requirement for Rubisco activase in diatoms*

A unique outcome of this study was the finding of the low and variable activation status of Rubisco in diatoms (~20–70%, Fig. 1) that implies a requirement for accessory factors for functional maintenance. As in higher plants, deactivation of diatom Rubisco probably results from loss of $Mg^{2+}$ and the carbamyl prosthetic group in the catalytic site, allowing for autoinhibition by substrate RuBP binding (to form 'ER' complexes). Likewise, binding of other inhibitory sugar phosphate molecules might occur to fully activated Rubisco (Andralojc *et al.*, 2012). Removal of the sugar phosphate is facilitated by Rubisco activase (RCA) via conformational remodeling driven by ATP hydrolysis (Mueller-Cajar *et al.*, 2014). In nature, differing types of RCA have independently evolved among plants, non-green algae (called CbbX; Mueller-Cajar *et al.*, 2013), and photosynthetic prokaryotes (called CbbOQ; Tsai *et al.*, 2016). While an RCA function in diatoms has not been demonstrated, they encode a chloroplast and nuclear *cbb*X gene (Kroth, 2015), consistent with our findings of a need for Rubisco activity regulation. The low activation status of diatom Rubisco somewhat parallels the low Rubisco activation status in $C_4$ plants (~40–60%; von Caemmerer and Furbank, 2003) and in $C_3$ plants grown at high $CO_2$ (e.g. it is <50% in tobacco grown in air containing 0.3% v/v $CO_2$; Whitney *et al.*, 1999). Understanding how the regulatory properties of diatom RCA and the activation status of Rubisco differ in response to environmental conditions (e.g. temperature, illumination, $CO_2$, and nutrients) and impact the resource use efficiency of diatoms have yet to be examined.

### *Photorespiration in diatoms*

Analogous to other Form I Rubisco (Savir *et al.*, 2010; Galmes *et al.*, 2014), diatom Form ID Rubisco showed a positive relationship between $K_C$ and $K_O$ (Fig. 3B). This indicates that unwanted reductions in $CO_2$ affinity (i.e. increasing $K_C$) are complemented by favorable reductions in $O_2$ affinity (i.e. increasing $K_O$). These kinetics help to ensure that the rates of photorespiration are not exacerbated in diatoms. The corresponding effect of specificity for $CO_2$ over $O_2$ ($S_{C/O}$) is quite variable, spanning values that match or exceed the $S_{C/O}$ of $C_3$ and $C_4$ plant Rubisco (Fig. 2E). As highlighted by Whitney *et al.* (2001), the lower carboxylation efficiencies under 21% $O_2$ ($k_{cat}^c/K_C^{21\%O2}$) shared by all diatom Rubiscos relative to plant Rubisco (Table 1) precludes them from being more efficient enzymes within the context of a $C_3$ plant chloroplast—irrespective of the higher $S_{C/O}$ values measured for some diatom Rubisco variants.

As in other CCM-containing organisms, the rates of photorespiration in diatoms will be suppressed under the higher $CO_2$ concentrations maintained around Rubisco in the pyrenoid. To date, however, little is known about the photorespiration process and rate in diatoms (Schnitzler Parker *et al.*, 2004; Rigobello-Masini *et al.*, 2012). As indicated above, resolving our understanding of diatom CCMs, and the $O_2$ levels in the pyrenoid, is vital to assessing the susceptibility of diatoms to photorespiration. One interpretation from the wide range in $K_O$ and $S_{C/O}$ values measured between the diatom species is that the $CO_2$:$O_2$ pressures within the pyrenoid may differ dramatically. This may arise through variation in the effectiveness of their CCM to concentrate $CO_2$ or through reduced permeability to $O_2$, or both. Particulaly curious is the elevated $O_2$ insensitivity (i.e. high $K_O$ value) of Rubisco from the centric diatom *T. weissflogii*. This suggests that there may be different biochemical constraints on the Rubisco in this species worthy of further study.

### *Conclusions*

Primary production in the oceans is dominated by phytoplankton, with diatoms accounting for ~20% of global primary production (Falkowski and Raven, 2007). Here we provide the largest data set of diatom Rubisco kinetics that identifies large

catalytic diversity and novel relationships in their properties. The data suggest that the CCM of diatoms is highly diverse and capable of concentrating $CO_2$ in the pyrenoid to higher levels than currently envisaged. Our findings also suggest that the $CO_2$ affinity of diatom Rubisco is a key indicator for how these microalgae manage the allocation of their relatively scarce cellular resources between Rubisco biogenesis and components of their CCM. This work highlights the importance of further studying the phylogenetically diverse, non-terrestrial, Rubisco isoforms to decipher potential mechanistic differences in the catalytic chemistry of the Form I Rubisco superfamily.

## Supplementary data

Supplementary data are available at *JXB* online.

Table S1. Rubisco kinetics at 25 °C taken from other data sets and used in Fig. 2

## Acknowledgements

We thank the reviewers for helpful comments that improved the article. Funding for JNY was through ANU visiting scholar (CE140100015) and NSF Grant 1040965. AH was funded through a Clarendon Scholarship, Oxford and ANU visiting scholar (CE140100015). RES was funded through ARC DECRA scheme (DE13010760). REMR was funded through ERC Starting Grant (SP2-GA-2008–200915), FMMM was funded through NSF Grant 104095, and SMW was funded through Australian Research Council Grant CE14010001

## References

**Andralojc PJ, Madgwick PJ, Tao Y, *et al***. 2012. 2-Carboxy-D-arabinitol 1-phosphate (CA1P) phosphatase: evidence for a wider role in plant Rubisco regulation. Biochemical Journal **442,** 733–742.

**Armstrong RA, Lee C, Hedges JI, Honjo S, Wakeham SG.** 2001. A new, mechanistic model for organic carbon fluxes in the ocean based on the quantitative association of POC with ballast minerals. Deep Sea Research Part II: Topical Studies in Oceanography **49,** 219–236.

**Badger MRT, Andrews J, Whitney SM, Ludwig M, Yellowlees DC, Leggat W, Price GD.** 1998. The diversity and coevolution of Rubisco, plastids, pyrenoids, and chloroplast-based $CO_2$-concentrating mechanisms in algae. Canadian Journal of Botany **76,** 1052–1071.

**Brown, JW. and Sorhannus, U.** (2010) A molecular genetic timescale for the diversification of autotrophic Stramenophiles (Ochrophyta): Substantive underestimation of putative fossil ages. PLoS ONE **5**(9):e12759.

**Carmo-Silva E, Scales JC, Madgwick PJ, Parry MAJ.** 2015. Optimizing Rubisco and its regulation for greater resource use efficiency. Plant, Cell and Environment **38,** 1817–1832.

**Chen X, Gao K.** 2004. Photosynthetic utilisation of inorganic carbon and its regulation in the marine diatom *Skeletonema costatum*. Functional Plant Biology **31,** 1027–1033.

**Delwiche CF, Palmer JD.** 1997. The origin of plastids and their spread via secondary symbiosis. In: Bhattacharya D, ed. The origins of algae and their plastids. Vienna: Springer-Verlag, 53–86.

**Egan KE, Rickaby REM, Hendry KR, Halliday AN.** 2013. Opening the gateways for diatoms primes Earth for Antarctic glaciation. Earth and Planetary Science Letters **375,** 34–43.

**Ehleringer JR, Cerling TE, Helliker BR.** 1997. $C_4$ photosynthesis, atmospheric $CO_2$, and climate. Oecologia **112,** 285–299.

**Falkowski P, Schofield O, Katz M, Van de Schootbrugge B, Knoll A.** 2004. Why is the land green and the ocean red? In: Thierstein H, Young J, eds. Coccolithophores. Berlin: Springer, 429–453.

**Falkowski PG, Raven JA.** 2007. Aquatic photosynthesis, Vol. **2**. Princeton, NJ: Princeton University Press.

**Furbank RT, Hatch MD.** 1987. Mechanism of $C_4$ photosynthesis: the size and composition of the inorganic carbon pool in bundle sheath cells. Plant Physiology **85,** 958–964.

**Galmes J, Kapralov MV, Andralojc PJ, Conesa MÀ, Keys AJ, Parry MAJ, Flexas J.** 2014. Expanding knowledge of the Rubisco kinetics variability in plant species: environmental and evolutionary trends. Plant, Cell and Environment **37,** 1989–2001.

**Ghannoum O, Evans JR, Chow WS, Andrews TJ, Conroy JP, von Caemmerer S.** 2005. Faster Rubisco is the key to superior nitrogen-use efficiency in NADP-malic enzyme relative to NAD-malic enzyme C(4) grasses. Plant Physiology **137,** 638–650.

**Giordano M, Beardall J, Raven JA.** 2005. $CO_2$ concentrating mechanisms in algae: mechanisms, environmental modulation, and evolution. Annual Review of Plant Biology **56,** 99–131.

**Haslam RP, Keys AJ, Andralojc PJ, Madgwick PJ, Andersson I, Grimsrud A, Eilertsen HC, Parry MAJ.** 2005. Specificity of diatom Rubisco. In: Omasa K, Nouchi I, De Kok LJ, eds. Plant responses to air pollution and global change. Springer: Japan, 157–164.

**Hauser T, Popilka L, Hartl FU, Hayer-Hartl M.** 2015. Role of auxiliary proteins in Rubisco biogenesis and function. Nature Plants **1,** 15065.

**Hennon GMM, Ashowrth J, Groussman RD, Berthiaume C, Morales RL, Baliga NS, Orellana MW, Armbrust EV.** 2015. Diatom acclimation to elevated $CO_2$ via novel gene clusters and cAMP-signaling. Nature Climate Change **5,** 761–765.

**Heureux AMC, Rickaby REM.** 2015. Refining our estimate of atmospheric $CO_2$ across the Eocene–Oligocene climatic transition. Earth and Planetary Science Letters **409,** 329–338.

**Hopkinson B.** 2014. A chloroplast pump model for the $CO_2$ concentrating mechanism in the diatom *Phaeodactylum tricornutum*. Photosynthesis Research **121,** 223–233.

**Hopkinson BM, Dupont CL, Allen AE, Morel FMM.** 2011. Efficiency of the $CO_2$-concentrating mechanism of diatoms. Proceedings of the National Academy of Sciences, USA **108,** 3830–3837.

**Hopkinson BM, Young JN, Tansik AL, Binder BJ.** 2014. The minimal $CO_2$-concentrating mechanism of *Prochlorococcus* spp. MED4 is effective and efficient. Plant Physiology **166,** 2205–2217.

**Kane HJ, Viil J, Entsch B, Paul K, Morell MK, Andrews TJ.** 1994. An improved method for measuring the $CO_2/O_2$ specificity of ribulose-bisphosphate carboxylase-oxygenase. Australian Journal of Plant Physiology **21,** 449–461.

**Kane HJ, Wilkin J-M, Portis AR, John Andrews T.** 1998. Potent inhibition of ribulose-bisphosphate carboxylase by an oxidized impurity in ribulose-1,5-bisphosphate. Plant Physiology **117,** 1059–1069.

**Kranz SA, Young JN, Hopkinson B, Goldman JAL, Tortell PD, Morel FMM.** 2015. Low temperature reduces the energetic requirement for the $CO_2$ concentrating mechanism in diatoms. New Phytologist **205,** 192–202.

**Kroth PG.** 2015. The biodiversity of carbon assimilation. Plant Physiology **172,** 76–81.

**Laing WA, Ogren WL, Hageman RH.** 1974. Regulation of soybean net photosynthetic $CO_2$ fixation by the interaction of $CO_2$, $O_2$, and ribulose 1,5-diphosphate carboxylase. Plant Physiology **54,** 678–685.

**Long BM, Bahar NHA, Atkin OK.** 2015. Contributions of photosynthetic and non-photosynthetic cell types to leaf respiration in *Vicia faba L.* and their responses to growth temperature. Plant, Cell and Environment **38,** 2263–2276.

**Long SP.** 1999. Environmental responses. In: Sage RF, Monson RK, eds. $C_4$ plant biology. Academic Press: San Diego, 215–249.

**Losh JL, Young JN, Morel FM.** 2013. Rubisco is a small fraction of total protein in marine phytoplankton. New Phytologist **198,** 52–58.

**Mueller-Cajar O, Stotz M, Bracher A.** 2014. Maintaining photosynthetic $CO_2$ fixation via protein remodelling: the Rubisco activases. Photosynthesis Research **119,** 191–201.

**Mueller-Cajar O, Whitney S.** 2008. Directing the evolution of Rubisco and Rubisco activase: first impressions of a new tool for photosynthesis research. Photosynthesis Research **98,** 667–675.

**Nakajima K, Tanaka A, Matsuda Y.** 2013. SLC4 family transporters in a marine diatom directly pump bicarbonate from seawater. Proceedings of the National Academy of Sciences, USA **110,** 1767–1772.

**Nelson DM, Tréguer P, Brzezinski MA, Leynaert A, Quéguiner B.** 1995. Production and dissolution of biogenic silica in the ocean: revised global estimates, comparison with regional data and relationship to biogenic sedimentation. Global Biogeochemical Cycles **9,** 359–372.

**Osborne CP, Sack L.** 2012. Evolution of $C_4$ plants: a new hypothesis for an interaction of $CO_2$ and water relations mediated by plant hydraulics.

Philosophical Transactions of the Royal Society B: Biological Sciences **367,** 583–600.

**Parry MAJ, Andralojc PJ, Scales JC, Salvucci ME, Carmo-Silva AE, Alonso H, Whitney SM.** 2013. Rubisco activity and regulation as targets for crop improvement. Journal of Experimental Botany **64,** 717–730.

**Peterhansel C, Niessen M, Kebeish RM.** 2008. Metabolic engineering towards the enhancement of photosynthesis. Photochemistry and Photobiology **84,** 1317–1323.

**Pierce J, Tolbert NE, Barker R.** 1980. Interaction of ribulose-bisphosphate carboxylase/oxygenase with transition-state analogues. Biochemistry **19,** 934–942.

**Price GD, Badger MR, Woodger FJ, Long BM.** 2008 Advances in understanding the cyanobacterial $CO_2$-concentrating-mechanism (CCM): functional components, Ci transporters, diversity, genetic regulation and prospects for engineering into plants. Journal of Experimental Botany **59,** 1441–1461.

**Price GD, Evans JR, von Caemmerer S, Yu J-W, Badger MR.** 1995. Specific reduction of chloroplast glyceraldehyde-3-phosphate dehydrogenase activity by antisense RNA reduces $CO_2$ assimilation via a reduction in ribulose bisphosphate regeneration in transgenic tobacco plants. Planta **195,** 369–378.

**Raven J, Beardall J, Giordano M.** 2014. Energy costs of carbon dioxide concentrating mechanisms in aquatic organisms. Photosynthesis Research **121,** 111–124.

**Raven J, Giordano M, Beardall J, Maberly SC.** 2011. Algal and aquatic plant carbon concentrating mechanisms in relation to environmental change. Photosynthesis Research **109,** 1–16.

**Raven JA.** 2009 Contributions of anyoxygenic and oxygenic phototrophy and chemolithotrophy to carbon and oxygen fluxes in aquatic environments. Aquatic Microbial Ecology **56,** 177–192.

**Raven JA, Beardall J.** 2016. The ins and outs of $CO_2$. Journal of Experimental Botany **67,** 1–13.

**Raven JA, Giordano M, Beardall J, Maberly SC.** 2012. Algal evolution in relation to atmospheric $CO_2$: carboxylases, carbon-concentrating mechanisms and carbon oxidation cycles. Philosophical Transactions of the Royal Society B: Biological Sciences **367,** 493–507.

**Read BA, Tabita FR.** 1994. High substrate specificity factor ribulose bisphosphate carboxylase/oxygenase from eukaryotic marine algae and properties of recombinant cyanobacterial rubisco containing 'algal' residue modifications. Archives of Biochemistry and Biophysics **312,** 210–218.

**Reinfelder JR.** 2010. Carbon concentrating mechanisms in eukaryotic marine phytoplankton. Annual Review of Marine Science **3,** 291–315.

**Reinfelder JR, Kraepiel AM, Morel FM.** 2000. Unicellular $C_4$ photosynthesis in a marine diatom. Nature **407,** 996–999.

**Reinfelder JR, Milligan AJ, Morel FMM.** 2004. The role of the $C_4$ pathway in carbon accumulation and fixation in a marine diatom. Plant Physiology **135,** 2106–2111.

**Rigobello-Masini M, Penteado JCP, Tiba M, Masini JC.** 2012. Study of photorespiration in marine microalgae through the determination of glycolic acid using hydrophilic interaction liquid chromatography. Journal of Separation Science **35,** 20–28.

**Roberts K, Granum E, Leegood RC, Raven JA.** 2007. Carbon acquisition by diatoms. Photosynthesis Research **93,** 79–88.

**Rost B, Riebesell U, Burkhardt S, Sültemeyer D.** 2003. Carbon acquisition of bloom-forming marine phytoplankton. Limnology and Oceanography **48,** 55–67.

**Sage RF.** 2001. Environmental and evolutionary preconditions for the origin and diversification of the $C_4$ photosynthetic syndrome. Plant Biology **3,** 202–213.

**Sage RF.** 2004. Tansley review: the evolution of $C_4$ photosynthesis. New Phytologist **161,** 341–371.

**Savir Y, Noor E, Milo R, Tlusty T.** 2010. Cross-species analysis traces adaptation of Rubisco toward optimality in a low-dimensional landscape. Proceedings of the National Academy of Sciences, USA **107,** 3475–3480.

**Schnitzler Parker M, Armbrust E, Piovia-Scott J, Keil RG.** 2004. Induction of photorespiration by light in the centric diatom *Thalassiosisra weissflogii* (Bacillariophyceae): molecular characterization and physiological consequences. Journal of Phycology **40,** 557–567.

**Seemann JR, Badger MR, Berry JA.** 1984. Variations in the specific activity of ribulose-1,5-bisphosphate carboxylase between species utilizing differing photosynthetic pathways. Plant Physiology **74,** 791–795.

**Sharwood RE, von Caemmerer S, Maliga P, Whitney SM.** 2008. The catalytic properties of hybrid rubisco comprising tobacco small and sunflower large subunits mirror the kinetically equivalent source rubiscos and can support tobacco growth. Plant Physiology **146,** 83–96.

**Sunda WG, Price NM, Morel FMM.** 2005. Trace metal ion buffers and their use in culture studies. In: Andersen RA, ed. Algal culturing techniques. Amsterdam: Elsevier, 35–63.

**Tabita FR, Satagopan S, Hanson TE, Kreel NE, Scott SS.** 2008. Distinct form I, II, III, and IV Rubisco proteins from the three kingdoms of life provide clues about Rubisco evolution and structure/function relationships. Journal of Experimental Botany **59,** 1515–1524.

**Tcherkez G.** 2013. Modelling the reaction mechanism of ribulose-1,5-bisphosphate carboxylase/oxygenase and consequences for kinetic parameters. Plant, Cell and Environment **36,** 1586–1596.

**Tcherkez G.** 2015. The mechanism of Rubisco-catalyzed oxygenation. Plant, Cell and Environment **39** (5), 983–997.

**Tcherkez GGB, Farquhar GD, Andrews TJ.** 2006. Despite slow catalysis and confused substrate specificity, all ribulose bisphosphate carboxylases may be nearly perfectly optimized. Proceedings of the National Academy of Sciences, USA **103,** 7246–7251.

**Tortell PD, Rau GH, Morel FM.** 2000. Inorganic carbon acquisition in coastal Pacific phytoplankton communities. Limnology and Oceanography **45,** 1485–1500.

**Tsai YC, Lapina MC, Bhushan S, Mueller-Cajar O.** 2016. Identification and characterization of multiple rubisco activases in chemoautotrophic bacteria. Nature Communications. **6,** 8883.

**von Caemmerer S, Furbank R.** 2003. The $C_4$ pathway: an efficient $CO_2$ pump. Photosynthesis Research **77,** 191–207.

**Way DA, Katul GG, Manzoni S, Vico G.** 2014. Increasing water use efficiency along the $C_3$ to $C_4$ evolutionary pathway: a stomatal optimization perspective. Journal of Experimental Botany **65,** 3683–3693.

**Whitehead L, Long BM, Price GD, Badger MR.** 2014. Comparing the in vivo function of $\alpha$-carboxysomes and $\beta$-carboxysomes in two model cyanobacteria. Plant Physiology **165,** 398–411.

**Whitney SM, Baldet P, Hudson GS, Andrews TJ.** 2001. Form I Rubiscos from non-green algae are expressed abundantly but not assembled in tobacco chloroplasts. The Plant Journal **26,** 535–547.

**Whitney SM, Houtz RL, Alonso H.** 2011. Advancing our understanding and capacity to engineer nature's $CO_2$-sequestering enzyme, Rubisco. Plant Physiology **155,** 27–35.

**Whitney SM, Sharwood RE.** 2007. Linked Rubisco subunits can assemble into functional oligomers without impeding catalytic performance. Journal of Biological Chemistry **282,** 3809–3818.

**Whitney SM, von Caemmerer S, Hudson GS, Andrews TJ.** 1999. Directed mutation of the Rubisco large subunit of tobacco influences photorespiration and growth. Plant Physiology **121,** 579–588.

**Yeoh H-H, Badger MR, Watson L.** 1980. Variations in $K_m(CO_2)$ of ribulose-1,5-bisphosphate carboxylase among grasses. Plant Physiology **66,** 1110–1112.

**Yoon HS, Hackett JD, Pinto G, Bhattacharya D.** 2002. The single, ancient origin of chromist plastids. Proceedings of the National Academy of Sciences, USA **99,** 15507–15512.

**Young JN, Bruggeman J, Rickaby REM, Erez J, Conte M.** 2013. Evidence for changes in carbon isotopic fractionation by phytoplankton between 1960 and 2010. Global Biogeochemical Cycles **27,** 505–515.

**Young JN, Kranz SA, Goldman JAL, Tortell PD, Morel FM.** 2015. Antarctic phytoplankton down-regulate their carbon concentrating mechanisms under high $CO_2$ with no change in growth rates. Marine Ecology Progress Series **532,** 13–28.

**Young JN, Rickaby REM, Kapralov MV, Filatov DA.** 2012. Adaptive signals in algal Rubisco reveal a hisotry of ancient atmospheric $CO_2$. Philosophical Transactions of the Royal Society B: Biological Sciences **367,** 483–492.

**Zelitch I, Schultes NP, Peterson RB, Brown P, Brutnell TP.** 2009. High glycolate oxidase activity is required for survival of maize in normal air. Plant Physiology **149,** 195–204.

**Zhu G, Jensen RG.** 1991. Xyulose 1,5-bisphosphate synthesized by ribulose 1,5-bisphosphate carboxylase/oxygenase during catalysis binds to decarbamylated enzyme. Plant Physiology **97,** 1348–1353.